FDTD modelling of velocity mismatch in travelling-wave heterojunction phototransistor

K.L. Tsakmakidis, L. Gomez-Rojas, I.D. Robertson, O. Hess, P.A. Houston and B. Weiss

Three-dimensional finite-difference time-domain modelling of a travelling-wave heterojunction phototransistor is presented. The electromagnetic model allows the simultaneous simulation of the optical and microwave properties of the travelling-wave structure. The results clearly demonstrate the effect of velocity mismatch between the optical wave and the photogenerated electrical wave.

Introduction: The use of heterojunction phototransistors (HPTs) in fibre-radio communication systems has attracted the interest of researchers for many years [1]. The device combines the functions of photodetection and amplification and is attractive for realising low-cost distribution points. As with the case of photodetectors, the 'travelling-wave' (TW) concept has been proposed and successfully demonstrated as a means of increasing the bandwidth and power-handling capability of an HPT. However, the development of optimum TW-HPT structures is still ongoing and, to understand fully the behaviour of such structures, a thorough modelling approach is essential.

This Letter presents a three-dimensional finite-difference time-domain (FDTD) electromagnetic modelling technique applied to a novel coplanar waveguide (CPW) InP TW-HPT structure. The device is similar to that reported by Prakash *et al.* [2], but with an integrated InAlGaAs optical waveguide. Both the optical and microwave properties of the device are investigated by taking full advantage of the FDTD method's full-wave nature. This is believed to be the first time that a complete numerical analysis of a travelling-wave photodetector structure has been reported. In other similar work in the relevant literature [3], only the microwave property was investigated and modelling was directed towards the accurate determination of the device's bandwidth. This Letter describes a different methodology for the modelling of the source compared to that in [3] or indeed in popular device simulation packages [4].

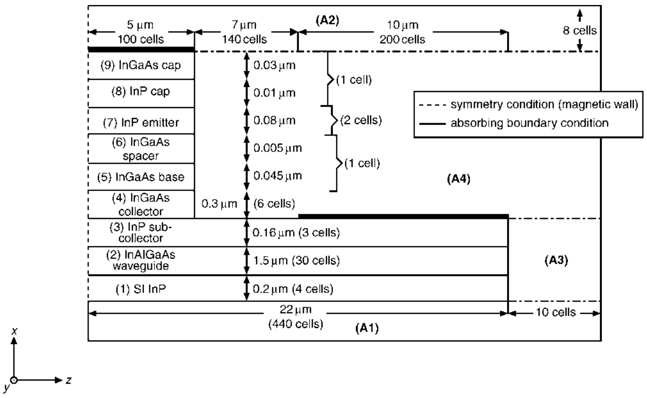

Fig. 1 *Cross-section of TW-HPT used in FDTD simulation*

A1, A2, A3 and A4 correspond to regions of air that surround the device

Device geometry and FDTD formulation: The device structure and details of the FDTD discretisation are shown in Fig. 1, and Table 1 lists the material parameters of each layer. The incorporation into the FDTD program of the very thin material sheets (InP cap and InGaAs spacer of thicknesses $d_1 = 0.01$ μm and $d_2 = 0.005$ μm, respectively) was carried out with the methodology found in [5], without any instabilities occurring. For the sake of brevity, only the value used for the 'averaged' conductivity in the updating of the E_y and E_z located exactly at the InGaAs cap/InP emitter interface is described in detail, and this is given by:

$$\sigma_{avg1} = \left(\frac{1}{2} - \frac{d_1}{\Delta x}\right)\sigma_{InGaAs-Cap} + \frac{d_1}{\Delta x}\sigma_{InP-Cap} + \frac{\sigma_{\text{InP-Emitter}}}{2}$$

In the microwave photonics area, and particularly for the simulation of photodetectors, the usual approach for the source modelling is to define a photocurrent source at specific grid points. For example, in [3] the presence of the propagating optical wave was incorporated into the FDTD algorithm by means of the photogenerated current density in the transverse direction that is produced by photogenerated electron-hole pairs. Similarly, in commercial simulation packages, such as the ATLAS^{TM} device simulation software from Silvaco [4], a photogeneration rate is defined at each grid point along the ray path, based on which an expression is derived for the photocurrent density. While this approach is, indeed, valid and can lead to accurate results it has one significant drawback: in a TW structure, it does not allow the simulation of the actual optical wave propagation inside its waveguide, and therefore results only for the microwave and not for the optical property of the device can be obtained.

Table 1: Device details

	ε_r	σ, S/m
SI InP	12.46	0
InAlGaAs waveguide	12.8881	0
InP sub-collector	12.46	160 200
InGaAs collector	13.88	162.6
InGaAs base	13.88	14 420
InGaAs spacer	13.88	0
InP emitter	12.46	29 480
InP cap	12.46	160 200
InGaAs cap	13.88	253 100

To simulate the propagation of the actual optical wave in such a structure, the source (usually Gaussian) must be assigned to one of the electric or magnetic field components inside the optical waveguide and the bandwidth of the excitation pulse should be well within the optical range of the signal spectrum. More importantly, the very small wavelengths present in the simulation domain necessitate the use of even smaller cell dimensions for the compensation of the numerical dispersion [5]. This is why in the FDTD simulation here, as opposed to the one in [3], we have used a very large 3D space-lattice ($60 \times 250 \times 450$ cells, Fig. 1) composed of very small cells (maximum dimension: 0.1 μm). For the quantitive investigation of the velocity mismatch between the optical and the electrical wave, such an approach is essential.

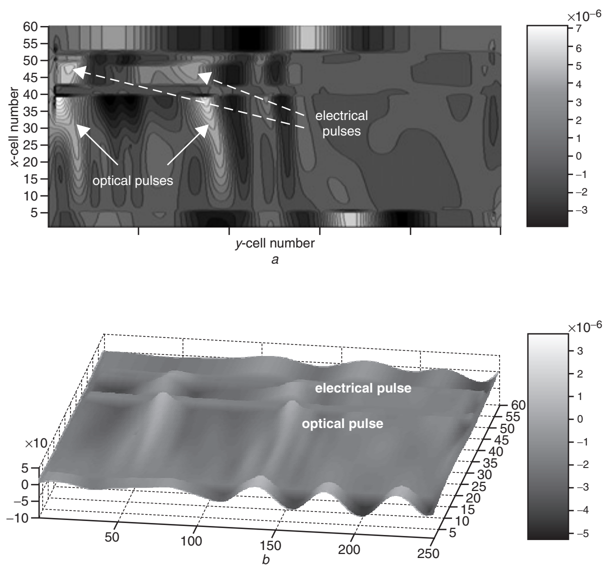

Fig. 2 *Snapshots of E_x-field spatial distribution at the z = 51 plane at two time steps*

a $n = 8500$. Clearly shows presence of two pairs of pulses; InP sub-collector separates optical and electrical waves. Pulses at left hand end are about to be reflected.
b $n = 10500$. In this snapshot, pulses have been reflected. Studying the right-hand pair of pulses, electrical pulse is clearly lagging significantly owing to velocity mismatch

Numerical results: In this study, the cell's dimensions were: $\Delta x = \Delta z = 0.05$ μm and $\Delta y = 0.1$ μm and $\Delta t = 2 \times 10^{-17}$ s was chosen for numerical stability reasons. The Mur first-order absorbing boundary condition (ABC) was applied at the five boundaries of the computational space and the 'magnetic wall' ($H_x = H_y = \partial E_z/\partial z = 0$) was used at the plane $z = 0$. The optical source was a Gaussian pulse with parameters $n_o = 0.07$ ps, $n_{decay} = 0.0095$ ps ($f_{\max} \cong 85$ THz) and was applied to the four E_x field components at the cells $(i,k) = (24-25, 50-51)$ at the $y = 45$ plane. Fig. 2 shows two snapshots of the E_x spatial distribution at the plane $z = 51$, which is perpendicular to the middle of the central metallic strip of Fig. 1. These snapshots clearly demonstrate the velocity mismatch between the optical and the photogenerated electrical pulses, the split of the electrical pulse into two equal parts travelling in opposite directions and the resulting waste of 50% of the photocurrent (if the reverse wave is terminated). The reflection of the electrical wave at the device's input results in two components for the total current. Fig. 3 shows the extracted effective refractive indices for the optical and electrical wave. It is found that $n_{\mathrm{opt.}} \cong 3.01$ and $n_{\mathrm{elect.}} \cong 3.2$, which agrees with the visual evidence of velocity-mismatch shown in Fig. 2.

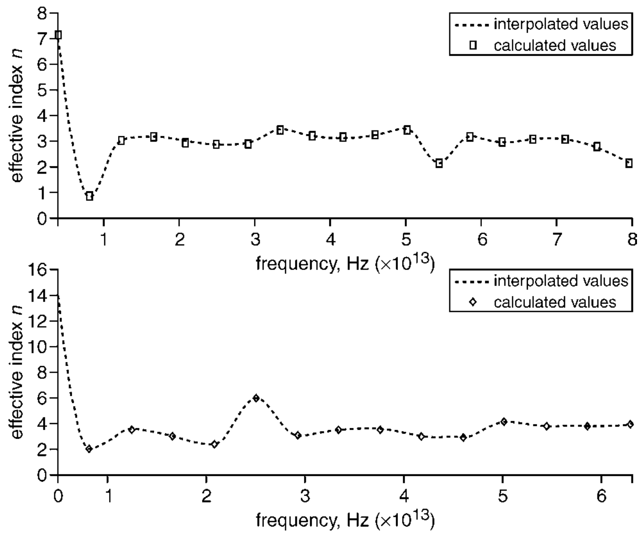

Fig. 3 *Effective refractive indices of optical and electrical wave*

DC-offset in low frequencies and peaks due to multimodal propagation
a Optical wave *b* Electrical wave

Conclusions: A three-dimensional FDTD electromagnetic model of a TW-HPT, enhanced with effective permittivity schemes and special techniques for the incorporation of thin material sheets, has been derived capable of indicating the main device characteristics, including optical absorption, microwave losses, as well as optical and microwave dispersion. Run in a parallel-processing machine, the numerical model provided useful and illuminating insight into the device's passive behaviour and clearly demonstrated the velocity mismatch between the optical wave and the microwave signal it generates.

Acknowledgment: This work is supported by EPSRC and is part of a collaborative project involving the Universities of Surrey, Leeds and Sheffield, and Bookham Technology.

29 January 2004
Electronics Letters online no: 20040248
doi: 10.1049/el:20040248

K.L. Tsakmakidis, L. Gomez-Rojas, I.D. Robertson, O. Hess and B. Weiss (*Advanced Technology Institute, University of Surrey, Guildford GU2 7XH, United Kingdom*)

P.A. Houston (*Department of Electronic and Electrical Engineering, University of Sheffield, United Kingdom*)

References

1 Campbell, J.C., and Ogawa, K.: 'Heterojunction phototransistors for long-wavelength optical receivers', *J. Appl. Phys.*, 1982, **53**, (2), pp. 1203–1208
2 Prakash, D.P., *et al.*: 'Integration of polyimide waveguides with travelling-wave phototransistors', *IEEE Photonics Technol. Lett.*, 1997, **9**, pp. 800–802
3 Kong, S.C., *et al.*: 'Numerical analysis of travelling-wave photodetectors' bandwidth using the finite-difference time-domain method', *IEEE Trans. Microw. Theory Tech.*, 2002, **50**, pp. 2589–2597
4 Atlas User's Manual: 'Device simulation software', Volume 1, 1998, Silvaco International
5 Taflove, A., and Hagness, S.C.: 'Computational electrodynamics: the finite-difference time-domain method' (Artech House, Boston and London, 2000, 2nd edn.)